2023 62nd IEEE Conference on Decision and Control (CDC)
December 13-15, 2023. Marina Bay Sands, Singapore

Data-driven Forward Stochastic Reachability Analysis for Human-in-the-Loop Systems

Joonwon Choi, Sooyung Byeon, and Inseok Hwang

***Abstract*— We propose a data-driven forward stochastic reachability analysis algorithm for Human-In-The-Loop (HITL) systems. We focus on a certain type of HITL system whose behavior is dominated by a human operator, for example, a multi-rotor controlled by a human operator. In such a system, the intervention of the human operator may generate a conservative reachable set due to the unpredictable control strategy of the human operator. The proposed algorithm computes a less conservative reachable set of the HITL system by accounting for the human operator's behavior, i.e., we present the data-driven reachability analysis algorithm that considers the unknown controller information of the HITL system. The behavior of the human operator is trained as a Gaussian Mixture Model (GMM) from the state and input trajectories of the system. Then, the conditional probability distribution of the human operator's behavior is obtained from the Gaussian Mixture Regression (GMR) for the closed-loop reachability analysis. The proposed algorithm is tested and demonstrated by the data collected from human subject experiments.**

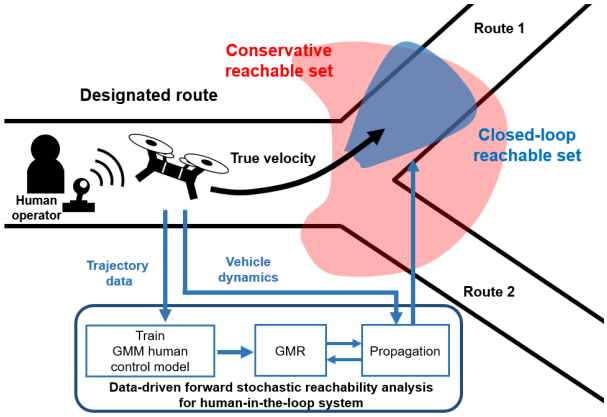

Fig. 1: Example of the HITL system with multiple control choices (routes) and the concept of the proposed algorithm

I. INTRODUCTION

The forward reachable set is a set of states at which a certain system can arrive at a specific future time instant. With the forward reachable set, one can verify the safety of the system by checking whether the reachable set violates safety constraints; or design a safety-guaranteeing controller [1]. However, the conventional reachability analysis methods may not be directly applicable, or if applicable, may yield inaccurate prediction results if the target system has an unknown element, for instance, a system lacking a mathematical model or controller information [2]. The data-driven reachability analysis has recently gained more attention as a solution for such systems that contain an unknown element. The data-driven reachability analysis can obtain the feasible reachable set by utilizing data generated by the system without requiring accurate knowledge about the target system [3].

In this paper, we aim to compute a reachable set for the Human-In-The-Loop (HITL) system controlled by a human operator. The reachability analysis has been widely used to guarantee the safety of the HITL system [4], [5]. Nevertheless, the closed-loop reachability analysis of the HITL system is challenging, as the behavior of the human operator is difficult to be modeled as a tractable form [6]. The lack of the controller (human operator) information could generate an overly conservative reachable set that is impractical for real-world applications or even degenerates the performance of the HITL system [7], [8]. The data-driven reachability analysis is required to alleviate the conservativeness of the reachable set by accounting for the behavior of the human operator.

Motivated by this, we propose a data-driven forward stochastic reachability analysis algorithm for the HITL systems. The proposed algorithm can reduce the conservativeness of the reachable set by realizing the closed-loop analysis. We assume that the behavior of the human operator is the only unknown element and the dynamics of the HITL system is given. Many existing data-driven reachability analysis methods mainly consider the system whose dynamics model is unavailable. It means that many existing methods are difficult to be directly applied to the closed-loop reachability analysis of the HITL system, as the unknown controller also needs to be considered. To tackle this problem, the proposed algorithm computes a less conservative reachable set by retrieving the behavior of the human operator from given data. We assume the dynamics of the system is given as a linear deterministic discrete-time system and the control input be given by the human operator. Note that this condition can be readily extended to the uncertain system with zero mean Gaussian noise whose control is input given by both a human and a machine.

The key challenge of computing the closed-loop reachable set in a data-driven manner is taking into account the human operator's behavior based on given data. To this end, we train the human operator's behavior as a form of the Gaussian Mixture Model (GMM) using the given control

The authors would like to acknowledge that this work is supported by NSF CNS-1836952

The authors with the School of Aeronautics and Astronautics, Purdue University, West Lafayette, IN 47907, USA {choi774, sbyeon, ihwang}@purdue.edu

2023 62nd IEEE Conference on Decision and Control (CDC) | 979-8-3503-0124-3/23/$31.00 ©2023 IEEE | DOI: 10.1109/CDC49753.2023.10383447

input trajectories and system state trajectories. The GMM has been widely applied to model a human driver's driving action [9] and to learn from demonstration of human motion [10]. The trained GMM human control model represents the joint probability distribution between the human operator's control input trajectory and system state trajectory. Then, the Gaussian Mixture Regression (GMR) provides the conditional probability distribution of the control input for a given system state, which can be regarded as a state feedback controller information of the HITL system. The stochastic reachable set, which is inferred as a probability density function (pdf) of the reachable state, is computed by propagating the state pdf and the result of the GMR. The proposed scheme can significantly reduce the conservativeness of the reachable set when the human operator has multiple choices, as shown in Fig. 1, by capturing the human operator's state dependent behavior.

The main contributions of this paper are as follows: (1) The data-driven forward stochastic reachability analysis algorithm for the HITL system is proposed, which can significantly reduce the conservativeness of the reachable set through the closed-loop analysis. Assuming HITL system's dynamics is known, the proposed algorithm accurately predicts the reachable set by explicitly accounting for the human operator's state dependent behavior; and (2) the proposed algorithm is tested and compared with some existing reachability analysis methods using the data collected from human subject experiments.

The rest of the paper is organized as follows: In Section II, the definition and method for training the GMM human control model are introduced. In Sections III and IV, the data-driven forward reachability analysis for the HITL system and the human subject experiment results are provided, respectively. Lastly, the conclusion is given in Section V.

II. GMM Human Control Model

In this paper, we assume the dynamics of the HITL system is given as a linear discrete-time system:

$$\boldsymbol{x}_{k+1} = A\boldsymbol{x}_k + B\boldsymbol{u}_k, \tag{1}$$

where $\boldsymbol{x}_k \in \mathbb{R}^n$ and $\boldsymbol{u}_k \in \mathbb{R}^m$ are the state and the control input vector at time step $k \in \mathbb{Z}$, respectively. $A \in \mathbb{R}^{n\times n}$ is the dynamics matrix and $B \in \mathbb{R}^{n\times m}$ is the input matrix. In this paper, we assume both A and B are known. In (1), the initial state ($\boldsymbol{x}_0$) has a Gaussian mixture uncertainty and $\boldsymbol{u}_k$ is assumed to be given by a human operator, i.e., the HITL system is driven by the human operator.

The objective of the proposed algorithm is to compute the pdf of the state at the desired future time step $T > 0$, $P(\boldsymbol{x}_T)$, by utilizing the GMM human control model. The GMM human control model is defined as a joint probability distribution between the system state trajectory and control input trajectory and contains the information about the human operator's state dependent behavior. In the following sections, we present how to construct the GMM human control model and extract the state feedback control information from the inferred GMM.

Remark 1: Although $\boldsymbol{u}_k$ is assumed to be given by the human operator in this paper, the same algorithm can be applied to a shared control system, where the machine and human operator share the same control space. Let $\boldsymbol{u}_k = \boldsymbol{u}_{h,k} + \boldsymbol{u}_{m,k}$, where $\boldsymbol{u}_{h,k}$ is the input from the human operator and $\boldsymbol{u}_{m,k}$ is the input from the machine. If $\boldsymbol{u}_{m,k}$ follows the linear state feedback law, i.e., $\boldsymbol{u}_{m,k} = K\boldsymbol{x}_k$ as in [11], where $K \in \mathbb{R}^{m\times n}$ is a proper gain matrix, the system dynamics (1) can be rewritten as

$$\begin{aligned}\boldsymbol{x}_{k+1} &= A\boldsymbol{x}_k + B(\boldsymbol{u}_{h,k} + \boldsymbol{u}_{m,k}) \\ &= (A + BK)\boldsymbol{x}_k + B\boldsymbol{u}_{h,k} \\ &= A'\boldsymbol{x}_k + B\boldsymbol{u}_{h,k}\end{aligned} \tag{2}$$

which has the same form as (1), where $A' = A + BK$.

A. Training GMM Human Control Model

The GMM is defined as a convex combination of multiple Gaussian distributions. Let the $i-$th Gaussian component of the GMM as $N(\boldsymbol{\mu}_{p,i}, \Sigma_{p,i})$ where $\boldsymbol{\mu}_{p,i}$ and $\Sigma_{p,i}$ are the mean and covariance, respectively. For the GMM with M Gaussian components, its pdf is represented as

$$\sum_{i=1}^{M} \pi_{p,i} N(\boldsymbol{\mu}_{p,i}, \Sigma_{p,i}), \tag{3}$$

where $\pi_{p,i}$ is the weight of each Gaussian component satisfying $\sum_{i=1}^{M} \pi_{p,i} = 1$.

The GMM (3) can be trained to represent the joint probability distribution between the state trajectory ($\boldsymbol{x}$) and the input trajectory ($\boldsymbol{u}$) of the system, $P(\boldsymbol{u}, \boldsymbol{x})$, where $\boldsymbol{u} = [\boldsymbol{u}_1^T, \boldsymbol{u}_2^T, \cdots, \boldsymbol{u}_{t_f}^T]^T$, $\boldsymbol{x} = [\boldsymbol{x}_1^T, \boldsymbol{x}_2^T, \cdots, \boldsymbol{x}_{t_f}^T]^T$, and t_f is the last time step of the trajectory. We train $P(\boldsymbol{u}, \boldsymbol{x})$ as the GMM human control model using the given trajectories of the HITL system. Let the augmented trajectory of the system be defined as $\boldsymbol{\zeta} = [\boldsymbol{\zeta}_0^T, \boldsymbol{\zeta}_1^T, \cdots, \boldsymbol{\zeta}_{t_f}^T]^T$, where $\boldsymbol{\zeta}_k = [\boldsymbol{u}_k^T, \boldsymbol{x}_k^T]^T$. Then, the proper parameters of the joint probability distribution $P(\boldsymbol{u}, \boldsymbol{x})$ can be computed by feeding $\boldsymbol{\zeta}$ to the Expectation Maximization (EM) algorithm [10].

Throughout the paper, we assume that the GMM human control model is composed of M Gaussian components and properly trained using a sufficient amount of data. In other words, $P(\boldsymbol{u}, \boldsymbol{x})$ is represented by the GMM in (3) which is trained by the sufficiently rich $\boldsymbol{\zeta}$.

B. Gaussian Mixture Regression (GMR)

After training the GMM human control model (3), one can compute the pdf of $\boldsymbol{u}_k$ when $\boldsymbol{x}_k$ is specified through the GMR, i.e., the conditional probability distribution of $\boldsymbol{u}_k$ for the given $\boldsymbol{x}_k$, $P(\boldsymbol{u}_k|\boldsymbol{x}_k)$, can be obtained by using (3) and the GMR [12]. $P(\boldsymbol{u}_k|\boldsymbol{x}_k)$ provides us the information about how the human operator would control the system for the given state, $\boldsymbol{x}_k$. By using $P(\boldsymbol{u}_k|\boldsymbol{x}_k)$ as the state-feedback controller information, we can realize the closed-loop stochastic reachability analysis of the HITL system.

Let $\boldsymbol{\mu}_{p,i}$ and $\Sigma_{p,i}$ in (3) be defined as

$$\boldsymbol{\mu}_{p,i} = \begin{pmatrix} \boldsymbol{\mu}_{p,i}^u \\ \boldsymbol{\mu}_{p,i}^x \end{pmatrix}, \Sigma_{p,i} = \begin{pmatrix} \Sigma_{p,i}^u & \Sigma_{p,i}^{ux} \\ \Sigma_{p,i}^{xu} & \Sigma_{p,i}^x \end{pmatrix}, \tag{4}$$

where $\boldsymbol{\mu}^u_{p,i} \in \mathbb{R}^m$ is the mean fraction corresponding to the human control input, $\boldsymbol{\mu}^x_{p,i} \in \mathbb{R}^n$ is that of the state, and $\Sigma^u_{p,i} \in \mathbb{R}^{m\times m}$, $\Sigma^x_{p,i} \in \mathbb{R}^{n\times n}$, $\Sigma^{ux}_{p,i} \in \mathbb{R}^{m\times n}$, and $\Sigma^{xu}_{p,i} \in \mathbb{R}^{n\times m}$ are the corresponding covariance fractions, respectively. Then, the conditional probability distribution $P(\boldsymbol{u}_k|\boldsymbol{x}_k)$ is computed as

$$P(\boldsymbol{u}_k|\boldsymbol{x}_k) = \sum_{i=1}^{M} \hat{\pi}_{p,i}(\boldsymbol{x}_k) N(\hat{\boldsymbol{\mu}}_{p,i}(\boldsymbol{x}_k), \hat{\Sigma}_{p,i}), \tag{5}$$

where

$$\hat{\boldsymbol{\mu}}_{p,i}(\boldsymbol{x}_k) = \boldsymbol{\mu}^u_{p,i} + \Sigma^{ux}_{p,i}{\Sigma^x_{p,i}}^{-1}(\boldsymbol{x}_k - \boldsymbol{\mu}^x_{p,i}), \tag{6}$$

$$\hat{\Sigma}_{p,i} = \Sigma^u_{p,i} - \Sigma^{ux}_{p,i}{\Sigma^x_{p,i}}^{-1}\Sigma^{xu}_{p,i}, \tag{7}$$

$$\hat{\pi}_{p,i}(\boldsymbol{x}_k) = \frac{\pi_{p,i} N(\boldsymbol{\mu}^x_{p,i}, \Sigma^x_{p,i})}{\sum_{j=1}^{M} \pi_{p,j} N(\boldsymbol{\mu}^x_{p,j}, \Sigma^x_{p,j})}. \tag{8}$$

In the following section, we present how to incorporate the GMR's output into the reachability analysis to achieve the closed-loop analysis.

III. Data-driven Forward Stochastic Reachability Analysis

A. Uncertainty Propagation of State and Control Input

One can compute the human operator's control input for the given state in the form of the conditional probability distribution using (5). Therefore, the pdf of the reachable state $P(\boldsymbol{x}_k)$ can be computed by propagating the state pdf and the conditional probability distribution of the human operator's control input (5) according to the given system dynamics (1).

Let us assume that the pdf of the state at time step k ($\boldsymbol{x}_k$) is represented as a GMM with L Gaussian components

$$P(\boldsymbol{x}_k) = \sum_{i=1}^{L} \pi_{k,i} N(\boldsymbol{\mu}_{k,i}, \Sigma_{k,i}), \tag{9}$$

where $\pi_{k,i}, \boldsymbol{\mu}_{k,i}$, and $\Sigma_{k,i}$ are the corresponding weight, mean, and covariance for the $i-$th Gaussian component, respectively. The propagation of the state pdf can be described by the Chapman-Kolmogorov equation [13]:

$$P(\boldsymbol{x}_{k+1}) = \int P(\boldsymbol{x}_{k+1}|\boldsymbol{x}_k) P(\boldsymbol{x}_k) d\boldsymbol{x}_k \tag{10}$$

By using (1), the conditional probability distribution $P(\boldsymbol{x}_{k+1}|\boldsymbol{x}_k)$ can be rewritten as

$$P(\boldsymbol{x}_{k+1}|\boldsymbol{x}_k) = P(A\boldsymbol{x}_k + B\boldsymbol{u}_k|\boldsymbol{x}_k). \tag{11}$$

Equation (11) shows the conditional probability distribution of the state at time step $k+1$ ($\boldsymbol{x}_{k+1}$) for the given current state ($\boldsymbol{x}_k$). When $\boldsymbol{x}_k$ is given, the pdf of the human operator's control input at the current time step can be computed from the GMR (5). By combining (5) with (11),

$$P(\boldsymbol{x}_{k+1}|\boldsymbol{x}_k) = \sum_{i=1}^{M} \hat{\pi}_{p,i}(\boldsymbol{x}_k) N(A\boldsymbol{x}_k + B\hat{\boldsymbol{\mu}}_{p,i}(\boldsymbol{x}_k), B\hat{\Sigma}_{p,i}B^T). \tag{12}$$

In (12), each Gaussian component's mean can be simplified as a linear function of $\boldsymbol{x}_k$. If we rewrite the $i-$th Gaussian component in (12) without the weight,

$$N(A\boldsymbol{x}_k + B\hat{\boldsymbol{\mu}}_{p,i}(\boldsymbol{x}_k), B\hat{\Sigma}_{p,i}B^T) = N(\bar{A}_i\boldsymbol{x}_k + \bar{B}_i, \bar{\Sigma}_i), \tag{13}$$

where

$$\begin{aligned} \bar{A}_i &= A + B\Sigma^{ux}_{p,i}{\Sigma^x_{p,i}}^{-1}, \\ \bar{B}_i &= B\boldsymbol{\mu}^u_{p,i} - B\Sigma^{ux}_{p,i}{\Sigma^x_{p,i}}^{-1}\boldsymbol{\mu}^x_{p,i}, \\ \bar{\Sigma}_i &= B\hat{\Sigma}_{p,i}B^T. \end{aligned} \tag{14}$$

Then, the new conditional probability distribution of $\boldsymbol{x}_{k+1}$ for the given $\boldsymbol{x}_k$ is represented with (12)-(14),

$$P(\boldsymbol{x}_{k+1}|\boldsymbol{x}_k) = \sum_{i=1}^{M} \hat{\pi}_{p,i}(\boldsymbol{x}_k) N(\bar{A}_i\boldsymbol{x}_k + \bar{B}_i, \bar{\Sigma}_i). \tag{15}$$

By substituting (15) for $P(\boldsymbol{x}_{k+1}|\boldsymbol{x}_k)$ in (10), we obtain

$$P(\boldsymbol{x}_{k+1}) = \int \sum_{i=1}^{M} \hat{\pi}_{p,i}(\boldsymbol{x}_k) N(\bar{A}_i\boldsymbol{x}_k + \bar{B}_i, \bar{\Sigma}_i) \cdot P(\boldsymbol{x}_k) d\boldsymbol{x}_k, \tag{16}$$

and by replacing $P(\boldsymbol{x}_k)$ with (9),

$$P(\boldsymbol{x}_{k+1}) = \int \sum_{i=1}^{M} \hat{\pi}_{p,i}(\boldsymbol{x}_k) N(\bar{A}_i\boldsymbol{x}_k + \bar{B}_i, \bar{\Sigma}_i) \cdot \sum_{j=1}^{L} \pi_{k,j} N(\boldsymbol{\mu}_{k,j}, \Sigma_{k,j}) d\boldsymbol{x}_k. \tag{17}$$

The inner part of (17) is described as a product of two GMMs, where one of the GMMs has $\hat{\pi}_{p,i}(\boldsymbol{x}_k)$ as its weight $\forall\, i = 1, 2, \cdots, M$. It is already proven that $P(\boldsymbol{x}_{k+1})$ is distributed by a GMM if $\hat{\pi}_{p,i}(\boldsymbol{x}_k)$ is constant $\forall\, i = 1, 2, \cdots, M$ [13]. Unfortunately, $P(\boldsymbol{x}_{k+1})$ might not be distributed by a GMM due to the state dependency in $\hat{\pi}_{p,i}(\boldsymbol{x}_k)$, which makes solving (17) intractable. To address this issue, we adopt a sampling-based propagation method [14] to propagate (17) in the following subsection.

Remark 2: The extension of the proposed algorithm to a system with zero mean Gaussian noise is trivial. Let the dynamics of the system be $\boldsymbol{x}_{k+1} = A\boldsymbol{x}_k + B\boldsymbol{u}_k + \boldsymbol{\omega}_k$, where $\boldsymbol{\omega}_k \in \mathbb{R}^n$ is the zero mean Gaussian system noise with zero mean vector $\mathbf{0} \in \mathbb{R}^n$ and covariance $\Sigma_k \in \mathbb{R}^{n\times n}$, $\boldsymbol{\omega}_k \sim N(\mathbf{0}, \Sigma_k)$. Then, the same algorithm can be applied by substituting $B\hat{\Sigma}_{p,i}B^T + \Sigma_k$ for $\bar{\Sigma}_i$ in (14).

B. Propagation through Sampling and Clustering

Although the pdf of the propagated state, $P(\boldsymbol{x}_{k+1})$, can be computed using (17), it is difficult to solve the equation

analytically. To tackle this problem, we use a sampling and clustering-based propagation method proposed in [14]. The method was originally used to approximate the prediction step of the Particle Gaussian Mixture (PGM) filter. In this paper, we apply the method to approximate (17). The algorithm starts by generating $N_s \in \mathbb{Z}^+$ samples ($S_s^i \in \mathbb{R}^n, i = 1, 2, \cdots, N_s$) from $P(\boldsymbol{x}_k)$ in (9). Then, one can generate $S_s^{'i} \in \mathbb{R}^n$ from the conditional probability distribution $P(\boldsymbol{x}_{k+1}|S_s^i)$ for each sample S_s^i using (15). $P(\boldsymbol{x}_{k+1})$ is approximated by clustering $S_s^{'i}$ as a GMM with L Gaussian components using a clustering algorithm such as the K-means. The detailed algorithm is presented in Algorithm 1.

Algorithm 1 Data-driven forward reachability analysis for HITL systems

Given the initial state $\boldsymbol{x}_0$ with initial GMM uncertainty, dynamics (1), trained GMM human control model (3), and desired future time step $T > 0$
$k \leftarrow 0$
while $k < T$ **do**
  $i \leftarrow 1$
  for $i < N_s + 1$ **do**
    Compute $\bar{A}_j, \bar{B}_j, \bar{\Sigma}_j, \forall j = 1, 2, \cdots, M$, using (14)
    $S_s^i \leftarrow$ samples from $P(\boldsymbol{x}_k)$ in (9)
    $S_s^{'i} \leftarrow$ samples from $P(\boldsymbol{x}_{k+1}|S_s^i)$ using (15) and $\bar{A}_j, \bar{B}_j, \bar{\Sigma}_j, \forall j = 1, 2, \cdots, M$
    $i \leftarrow i + 1$
  end for
  $P(\boldsymbol{x}_{k+1}) \leftarrow$ GMM with L Gaussian components clustered from $S_s^{'i}, \forall i = 1, 2, \cdots, N_s$
  $k \leftarrow k + 1$
end while

IV. Human Subject Experiment

A. Simulation Setup

To test the performance of the proposed algorithm, we first trained the GMM human control model using the trajectories obtained from human subject experiments[1]. The scenario used for the experiment is shown in Fig. 2. In the experiment, the participant should safely land a multi-rotor vehicle on the goal point in the 2-D simulation environment. The vehicle should maintain its speed as $10[m/s]$ and follow one of the designated routes, left or right, which was informed at the beginning of each trial. By training the GMM human control model using the recorded flight trajectories, we try to validate whether the proposed algorithm can distinguish the human operator's designated route based on the given state of the vehicle; and achieve a less conservative but accurate reachable set of the HITL system. A total of 150 trajectories were collected, 75 for each route, and 145 of them were used to train the GMM. The remaining 5 trajectories were used for validation.

[1]The Institutional Review Board (IRB) at Purdue University approved the study. IRB protocol number: IRB-2020-755.

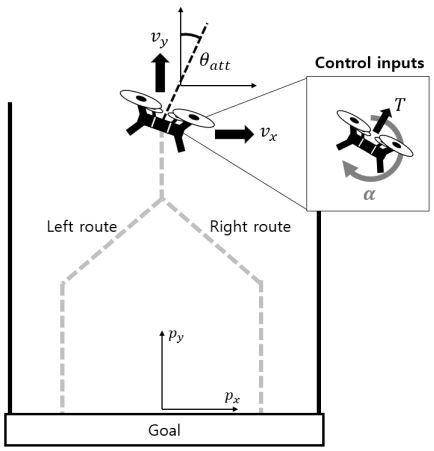

Fig. 2: Simulation scenario

For the multi-rotor vehicle's dynamics, we define the system matrices A and B in (1) as follow:

$$A = I_6 + \begin{pmatrix} 0 & 0 & 0 & 1 & 0 & 0 \\ 0 & 0 & 0 & 0 & 1 & 0 \\ 0 & 0 & 0 & 0 & 0 & 1 \\ 0 & 0 & g & 0 & 0 & 0 \\ 0 & 0 & 0 & 0 & k_1 & 0 \\ 0 & 0 & k_2 & 0 & 0 & k_3 \end{pmatrix} \Delta t, \tag{18}$$

$$B = \begin{pmatrix} 0 & 0 \\ 0 & 0 \\ 0 & 0 \\ 0 & 0 \\ 0 & 1/m \\ 1/I_x & 0 \end{pmatrix} \Delta t, \tag{19}$$

where Δt is the discretization time interval, g is the gravitational acceleration, m and I_x are the mass and the moment of inertia of the multi-rotor, respectively; k_1, k_2, and k_3 are the controller parameters; and I_6 is the 6×6 identity matrix. A and B are obtained by linearizing the multi-rotor's dynamics with respect to a hovering point [15]. The state vector $\boldsymbol{x}_k \in \mathbb{R}^6$ is defined as $\boldsymbol{x}_k = [p_{x,k}, p_{y,k}, \theta_{att,k}, v_{x,k}, v_{y,k}, \dot{\theta}_k]^T$, which consists of the X and Y axis position $(p_{x,k}, p_{y,k})$, the attitude $(\theta_{att,k})$, the X and Y axis linear velocity $(v_{x,k}, v_{y,k})$, and the angular velocity $(\dot{\theta}_{att,k})$ at time step k. The control

TABLE I: Simulation parameters

Discretization time interval (Δt)	0.1 $[s]$
Gravitational acceleration (g)	9.8 $[m/s^2]$
Mass (m)	0.25 $[kg]$
Moment of inertia (I_x)	0.01 $[kg \cdot m^2]$
Control parameter (k_1, k_2, k_3)	$-0.1, -1, -30$
Thrust input bound (T)	$[-1.5, 1.5]$
Angular acceleration input bound (α)	$[-0.5, 0.5]$
X axis speed bound (v_x)	$[-10, 10][m/s]$
Y axis speed bound (v_y)	$[-15, 15][m/s]$
Gaussian components for human control model (M)	6
Gaussian components for state pdf (L)	6
Number of samples for comparative methods	2500
Number of samples for propagation of (17) (N_s)	1500

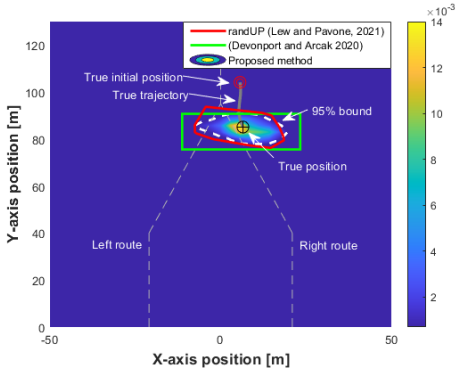

(a) $T = 2$ $[s]$

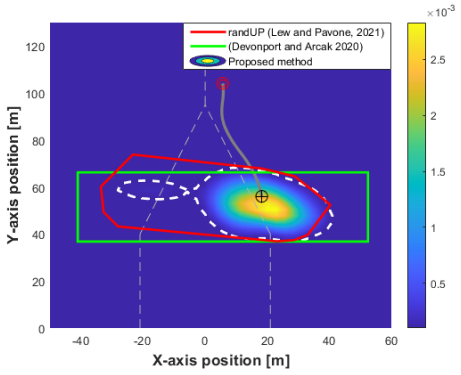

(b) $T = 5$ $[s]$

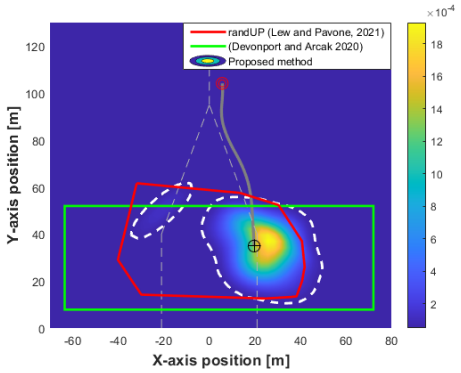

(c) $T = 7$ $[s]$

Fig. 3: Comparative simulation results when the multi-rotor is heading toward the right route

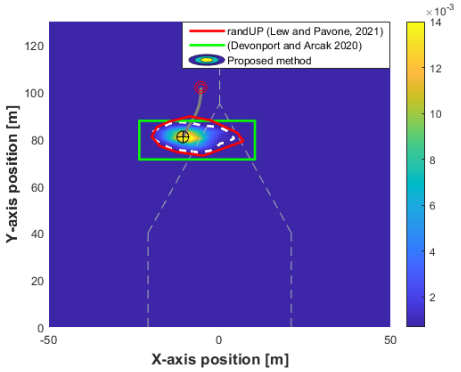

(a) $T = 2$ $[s]$

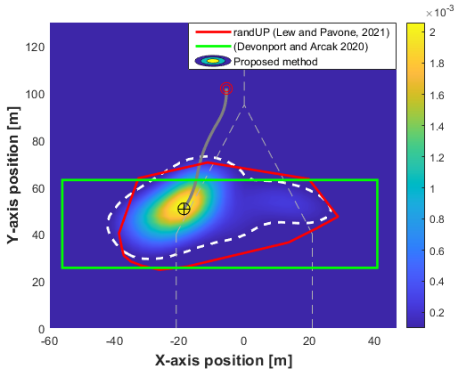

(b) $T = 5$ $[s]$

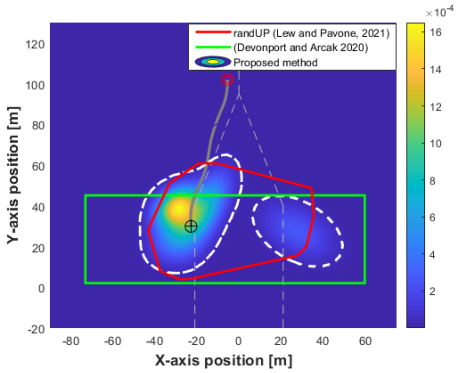

(c) $T = 7$ $[s]$

Fig. 4: Comparative simulation results when the multi-rotor is heading toward the left route

input $\boldsymbol{u}_k \in \mathbb{R}^2$ is defined as $\boldsymbol{u}_k = [\alpha_k, T_k]^T$ where α_k and T_k are the angular acceleration and the thrust at time step k, respectively. For the initial state, $\boldsymbol{x}_0$, we assume there is the initial single Gaussian uncertainty $N(\mathbf{0}, \Sigma_0)$ where $\Sigma_0 = diag[1.5, 1.5, 0.1, 0.5, 1, 0.1]$.

The augmented trajectory used for the GMM human control model training is defined as

$$\boldsymbol{\zeta} = [\boldsymbol{\zeta}_0^T, \boldsymbol{\zeta}_1^T, \cdots, \boldsymbol{\zeta}_{t_f}^T]^T \tag{20}$$

where

$$\boldsymbol{\zeta}_k = [\alpha_k, T_k, p_{x,k}, p_{y,k}, \theta_{att,k}, v_{x,k}, v_{y,k}, \dot{\theta}_{att,k}]^T, \tag{21}$$

with t_f as the last time step of the trajectory. We separated 6 $[s]$ of the trajectory for each trial and constructed $\boldsymbol{\zeta}$ by concatenating them. The detailed parameters used for the simulation can be found in Table I.

We compare our proposed algorithm's result with other existing reachability analysis methods. For a fair comparison, we borrow two algorithms that can account for the trained GMM human control model: randUP [16] and the Monte Carlo sampling-based method proposed in [17]. Both of the algorithms propagate the state by sampling from the trained GMM human control model and the number of samples is set to be 2500. All the pdfs are properly marginalized or

truncated depending on the conditions.

B. Simulation Result

Fig. 3 and 4 show the simulation results of the proposed algorithm and the other two existing algorithms. In the figures, the red circle indicates the true initial position of the multi-rotor, where we start the prediction, the dark gray line is the true trajectory, and the black circle is the true position of the multi-rotor at a specific time instant. The gray dashed line shows the simulation routes that are described in Fig. 2. The proposed algorithm's results are plotted as contours where the brighter line means the higher probability of the multi-rotor to be located. Besides, the 95% level-set boundary of the proposed algorithm is indicated by the white dashed line, which can be regarded as the $\epsilon-$accurate reachable set proposed in [17]. Meanwhile, the results of randUP [16] and the Monte Carlo sampling-based method [17] are represented as the red and the green line, respectively.

Fig. 3(a)-3(c) and 4(a)-4(c) show the trajectories of the multi-rotor from 2 [s] to 7 [s] in to the future after the prediction begins. From the figures, one can easily notice that the existing methods generate conservative reachable sets which include both of the routes, i.e., they cannot accurately predict which route the multi-rotor will follow. This result might be impractical in real-world applications as the reachable set cannot distinguish the human operator's control choice. For instance, for a car crossing an intersection, such a conservative reachable set covers the other corners that the car is not actually heading toward. This yields the risk to be overestimated and impedes the analysis by taking into account unnecessary factors, which the human operator scarcely encounters in practice. In contrast, the proposed algorithm successfully predicts the route where the multi-rotor is heading by giving more probability weight to it; and thus can significantly reduce the conservativeness of the reachable set by explicitly accounting for the human operator's behavior using the GMM human control model. This characteristic provides significant benefits to the HITL system by preventing unnecessary interruption from the machine, for example, making an assistant system intervene only when the human operator is truly in danger; or reducing false alarms of a warning system to preserve the reliance on the system [9].

V. Conclusion

In this paper, we proposed the data-driven forward stochastic reachability analysis method for the Human-In-The-Loop (HITL) system, which can significantly alleviate the conservativeness of the reachable set through the closed-loop analysis. Our proposed algorithm trains the Gaussian Mixture Model (GMM) human control model from the given trajectories of the HITL system and computes the expected human operator's control probability density function (pdf) using the Gaussian Mixture Regression (GMR). The proposed algorithm computes the pdf of the state at desired future time step by propagating the GMR result according to the given dynamics. Through the human subject experiment, the computed reachable set is shown to be less conservative than the reachable sets computed by two existing algorithms, which can be achieved by explicitly considering the human operator's state feedback behavior.

References

[1] A. P. Vinod, B. HomChaudhuri, and M. M. Oishi, "Forward stochastic reachability analysis for uncontrolled linear systems using Fourier transforms," in *Proceedings of the 20th International Conference on Hybrid Systems: Computation and Control*, 2017, pp. 35–44.

[2] A. J. Thorpe and M. M. Oishi, "Model-free stochastic reachability using kernel distribution embeddings," *IEEE Control Systems Letters*, vol. 4, no. 2, pp. 512–517, 2019.

[3] A. Alanwar, A. Koch, F. Allgöwer, and K. H. Johansson, "Data-driven reachability analysis from noisy data," *arXiv preprint arXiv:2105.07229*, 2021.

[4] X.-M. Zhang and H.-N. Wu, "Reachable set estimation of a class of human-in-the-loop control systems," in *2021 40th Chinese Control Conference (CCC)*, 2021, pp. 1083–1087.

[5] K. Leung, E. Schmerling, M. Zhang, M. Chen, J. Talbot, J. C. Gerdes, and M. Pavone, "On infusing reachability-based safety assurance within planning frameworks for human-robot vehicle interactions," *The International Journal of Robotics Research*, vol. 39, no. 10-11, pp. 1326–1345, 2020.

[6] V. Govindarajan, K. Driggs-Campbell, and R. Bajcsy, "Data-driven reachability analysis for human-in-the-loop systems," in *2017 IEEE 56th Annual Conference on Decision and Control (CDC)*, 2017, pp. 2617–2622.

[7] A. Pereira and M. Althoff, "Overapproximative human arm occupancy prediction for collision avoidance," *IEEE Transactions on Automation Science and Engineering*, vol. 15, no. 2, pp. 818–831, 2017.

[8] K. Driggs-Campbell, R. Dong, and R. Bajcsy, "Robust, informative human-in-the-loop predictions via empirical reachable sets," *IEEE Transactions on Intelligent Vehicles*, vol. 3, no. 3, pp. 300–309, 2018.

[9] P. Angkititrakul, R. Terashima, and T. Wakita, "On the use of stochastic driver behavior model in lane departure warning," *IEEE Transactions on Intelligent Transportation Systems*, vol. 12, no. 1, pp. 174–183, 2010.

[10] S. Calinon, "A tutorial on task-parameterized movement learning and retrieval," *Intelligent Service Robotics*, vol. 9, no. 1, pp. 1–29, 2016.

[11] S. Byeon, D. Sun, and I. Hwang, "Skill-level-based hybrid shared control for human-automation systems," in *2021 IEEE International Conference on Systems, Man, and Cybernetics (SMC)*, 2021, pp. 1507–1512.

[12] F. Stulp and O. Sigaud, "Many regression algorithms, one unified model: A review," *Neural Networks*, vol. 69, pp. 60–79, 2015.

[13] A. Karumanchi and P. Tulpule, "Comparing linear systems with Gaussian mixture model additive uncertainties using Kullback-Leibler rate," *IFAC-PapersOnLine*, vol. 54, no. 20, pp. 566–572, 2021.

[14] D. Raihan and S. Chakravorty, "Particle Gaussian mixture filters-I," *Automatica*, vol. 98, pp. 331–340, 2018.

[15] F. Sabatino, "Quadrotor control: modeling, nonlinear control design, and simulation," *Master thesis, KTH Royal Institute of Technology*, 2015.

[16] T. Lew and M. Pavone, "Sampling-based reachability analysis: A random set theory approach with adversarial sampling," in *Conference on Robot Learning*, 2021, pp. 2055–2070.

[17] A. Devonport and M. Arcak, "Data-driven reachable set computation using adaptive Gaussian process classification and Monte Carlo methods," in *2020 American Control Conference (ACC)*, 2020, pp. 2629–2634.